Identification of a Novel Class of Small-Molecule Antiangiogenic Agents through the Screening of Combinatorial Libraries Which Function by Inhibiting the Binding and Localization of Proteinase MMP2 to Integrin $\alpha_V\beta_3$

Dale L. Boger,*,† Joel Goldberg,† Steve Silletti,‡,§ Torsten Kessler,‡ and David A. Cheresh‡

Contribution from the Departments of Chemistry, Immunology, and Vascular Biology and The Skaggs Institute for Chemical Biology, The Scripps Research Institute, 10550 North Torrey Pines Road, La Jolla, California 92037

Received October 3, 2000

Abstract: The process of new blood vessel growth from existing vasculature, known as angiogenesis, is critical to several pathological conditions, most notably cancer. Both MMP2, which degrades the extracellular matrix (ECM), and integrin $\alpha_V\beta_3$, which contributes to endothelial cell attachment to the ECM, are critically involved in this process. Recent findings have shown that MMP2 is localized in an active form on the surface of invasive endothelial cells based on its ability to directly bind integrin $\alpha_V\beta_3$, suggesting that disrupting this protein−protein interaction may represent a new target for the development of angiogenesis inhibitors. The screening of small molecule libraries led to the identification of compounds which disrupt the MMP2−$\alpha_V\beta_3$ interaction in an in vitro binding assay. A prototypical inhibitor was further found to prevent the degradation of the protein matrix without directly inhibiting MMP2 activity or disrupting the binding of $\alpha_V\beta_3$ to its classical ECM ligand, vitronectin. The synthesis and screening of analogues and substructures of this lead compound allowed the identification of requisite structural features for inhibition of MMP2 binding to $\alpha_V\beta_3$. This led to the synthesis of a more water-soluble derivative which maintains the in vitro biological properties and has potent antiangiogenic and antitumor activity in vivo, validating the target as one useful for therapeutic intervention.

Introduction

The development of new blood vessels from existing vasculature, a process known as angiogenesis, has been the subject of considerable research.[1] This process is normally involved in wound repair, inflammation, and embryonic development, whereas aberrant angiogenesis is characteristic of several pathological conditions,[2] including arthritis, ocular retinopathy, and tumor growth and metastasis.[3] Progress in recent years has led to a better understanding of angiogenesis, revealing that it is a multistep process involving vascular cell activation, matrix degradation, and cell migration, proliferation, and differentiation. A number of proteolytic enzymes and cell-surface receptors are involved, and the process can be promoted or inhibited by the action of growth factors and other endogenous regulators.[4] Several approaches, targeting angiogenesis at different stages, are being pursued as potential cancer therapies. Recent estimates indicate that at least 40 pharmaceutical firms are developing angiogenesis inhibitors with at least 27 drugs currently in clinical trials.[5]

MMP2 (gelatinase A), a member of the matrix metalloproteinase family, is secreted by vascular endothelial cells and plays a crucial role in degrading the extracellular matrix (ECM) during tumor-induced angiogenesis.[6] Peptide and peptidomimetic MMP2 inhibitors have been developed which diminish tumor growth and metastasis.[7] Another key participant in angiogenesis is the integrin $\alpha_V\beta_3$, which mediates cellular interactions with the ECM.[8] This heterodimeric cell-surface protein recognizes certain matrix proteins containing the RGD (Arg-Gly-Asp) peptide sequence, leading to integrin clustering and ultimately supporting endothelial cell migration and survival. Soluble RGD peptides, nonpeptide RGD mimetics, and antibodies that disrupt $\alpha_V\beta_3$ ligation have been shown to inhibit angiogenesis.[9] In addition, a number of investigators have developed antagonists of integrin $\alpha_{IIb}\beta_3$, which plays a key role in thrombosis and platelet aggregation,[10] some of which are currently approved for thrombotic disease. Because of the similarity of the ligands recognized by the different integrins, an inherent obstacle in the design of effective $\alpha_V\beta_3$ antagonists for use in antiangiogenic therapy is integrin selectivity (e.g., $\alpha_V\beta_3$ vs $\alpha_{IIb}\beta_3$).

Recently, a novel interaction between MMP2 and integrin $\alpha_V\beta_3$ was observed when these proteins were found to colocalize on the surface of angiogenic blood vessels in vivo.[11] Integrin

† Department of Chemistry and The Skaggs Institute for Chemical Biology.

‡ Departments of Immunology and Vascular Biology.

§ Current address: Department of Pediatrics−Whitier Institute, University of California, San Diego, 9894 Genesee Ave., La Jolla, CA 92037.

(1) Klagsbrun, M.; Moses, M. A. *Chem. Biol.* **1999**, *6*, R217.

(2) Folkman, J. *Nature Med.* **1995**, *1*, 27.

(3) Folkman, J. *New Engl. J. Med.* **1971**, *285*, 1182.

(4) Fan, T.-P. D.; Jaggar, R.; Bicknell, R. *Trends Pharmacol. Sci.* **1995**, *16*, 57.

(5) Brower, V. *Nature Biotechnol.* **1999**, *17*, 963. Klohs W. D.; Hamby J. M. *Curr. Opin. Biotechnol.* **1999**, *10*, 544.

(6) Chen, J.-M.; Aimes, R. T.; Ward, G. R.; Youngleib, G. L.; Quigley, J. P. *J. Biol. Chem.* **1991**, *266*, 5113.

(7) Kahari, V.-M.; Saarialho-Kere, U. *Ann. Med.* **1999**, *31*, 34.

(8) Brooks, P. C.; Clark, R. A. F.; Cheresh, D. A. *Science* **1994**, *264*, 569. For a review of endogenous ligand binding to integrins, see: Plow, E. F.; Haas, T. A.; Zhang, L.; Loftus, J.; Smith, J. W. *J. Biol. Chem.* **2000**, *275*, 21785.

(9) Giannis, A.; Rubsam, F. *Angew. Chem., Int. Ed. Engl.* **1997**, *36*, 588.

(10) Eldred, C. D.; Judkins, B. D. *Prog. Med. Chem.* **1999**, *36*, 29.

10.1021/ja003579+ CCC: $20.00
Published on Web 01/26/2001

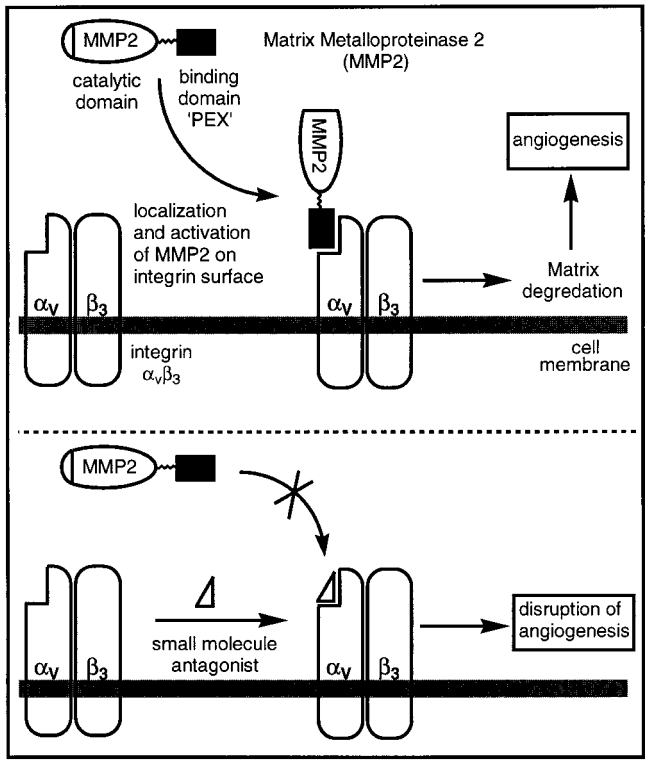

Figure 1. Top: Depiction of the MMP2−$\alpha_V\beta_3$ interaction and its role in angiogenesis. Bottom: A small-molecule antagonist can disrupt angiogenesis by inhibiting the localization of MMP2 to the cell surface through binding to $\alpha_V\beta_3$.

$\alpha_V\beta_3$ binds MMP2, and this interaction is a requisite step in the cellular utilization of the enzyme on the surface of invasive endothelial cells.[12] A noncatalytic, 193 residue C-terminal fragment of MMP2, termed PEX, was found to inhibit MMP2 binding to $\alpha_V\beta_3$ and to indirectly block its cell surface proteolytic activity.[13] PEX was further shown to disrupt angiogenesis and tumor growth in the chick chorioallantoic membrane. A naturally occurring form of PEX can be detected in vivo in association with cells expressing $\alpha_V\beta_3$, suggesting its role as an endogenous regulator of angiogenesis. These observations indicate that disrupting the binding of MMP2 to integrin $\alpha_V\beta_3$ may be a promising approach to controlling angiogenesis and could lead to novel therapeutic agents for angiogenesis-dependent diseases including cancer (Figure 1).

The exact nature of the MMP2−$\alpha_V\beta_3$ interaction is unknown, although it has been established that the integrin binding site is distinct from that which recognizes the RGD sequence in traditional high-affinity ligands (e.g., vitronectin).[12] Without further knowledge of the target structure available, a combinatorial chemistry[14] approach was undertaken in search of small molecule MMP2−$\alpha_V\beta_3$ antagonists. Herein we report the discovery of the first members of a new class of antiangiogenic compounds that derive their activity by inhibiting this protein−protein interaction and validate this target as a useful one for therapeutic intervention.

We have previously described solution phase methodology designed for the generation of chemical libraries suitable for studying protein−protein interactions.[15,16] This approach allows for the rapid generation of multimilligram quantities of combinatorial mixtures and individual compounds with two or more binding groups separated by variable linkers that can interact with one or more protein targets. The screening of such compound libraries as antagonists of the MMP2−$\alpha_V\beta_3$ interaction was undertaken to identify lead compounds as potential angiogenesis inhibitors. As described in the following sections, this led to the initial identification of **1** (**A6B10C4**), its refinement to **19**, and its subsequent simplification to provide **34** which also possesses improved solubility and in vivo activity (Figure 2).

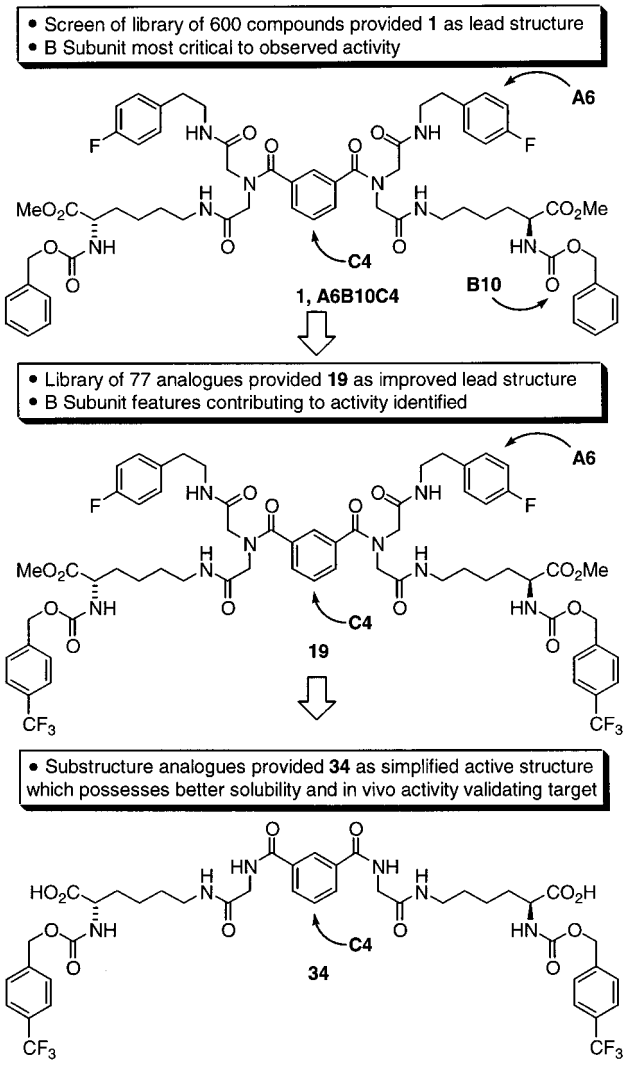

Figure 2.

Library Screening Results. Mixture library **1** was found to have antagonist activity in an assay which measures the in vitro binding of MMP2 to $\alpha_V\beta_3$. This library consists of 600 symmetrical dimeric structures which contain three diversity subunits (Figure 3). The library was synthesized by combining

(11) Brooks, P. C.; Strömblad, S.; Sanders, L. C, von Schalscha, T. L.; Aimes, R. T.; Stetler-Stevenson, W. G.; Quigley, J. P.; Cheresh, D. A. *Cell* **1996**, *85*, 683.
(12) Silletti, S.; Cheresh, D. A. *Fibrinolysis Proteolysis* **1999**, *13*, 226.
(13) Brooks, P. C.; Silletti, S.; von Schalscha, T. L.; Friedlander, M.; Cheresh, D. A. *Cell* **1998**, *92*, 391.
(14) Floyd, C. D.; Leblanc, C.; Whittaker, M. *Prog. Med. Chem.* **1999**, *36*, 91.
(15) Boger, D. L.; Goldberg, J.; Jiang, W.; Chai, W.; Ducray, P.; Lee, J. K.; Ozer, R. S.; Andersson, C.-M. *Bioorg. Med. Chem.* **1998**, *6*, 1347.
(16) Cheng, S.; Comer, D. D.; Williams, J. P.; Boger, D. L. *J. Am. Chem. Soc.* **1996**, *118*, 2567. Boger, D. L.; Tarby, C. M.; Caporale, L. H. *J. Am. Chem. Soc.* **1996**, *118*, 2109. Cheng, S.; Tarby, C. M.; Comer, D. D.; Williams, J. P.; Caporale, L. H.; Boger, D. L. *Bioorg. Med. Chem.* **1996**, *4*, 727. Boger, D. L.; Ducray, P.; Chai, W.; Jiang, W.; Goldberg, J. *Bioorg. Med. Chem. Lett.* **1998**, *8*, 2339. Boger, D. L.; Ozer, R. S.; Andersson, C.-M. *Bioorg. Med. Chem. Lett.* **1997**, *7*, 1903. Boger, D. L.; Chai, W. *Tetrahedron* **1998**, *54*, 3955. Boger, D. L.; Chai, W.; Ozer, R. S.; Andersson, C.-M. *Bioorg. Med. Chem. Lett.* **1997**, *7*, 463.

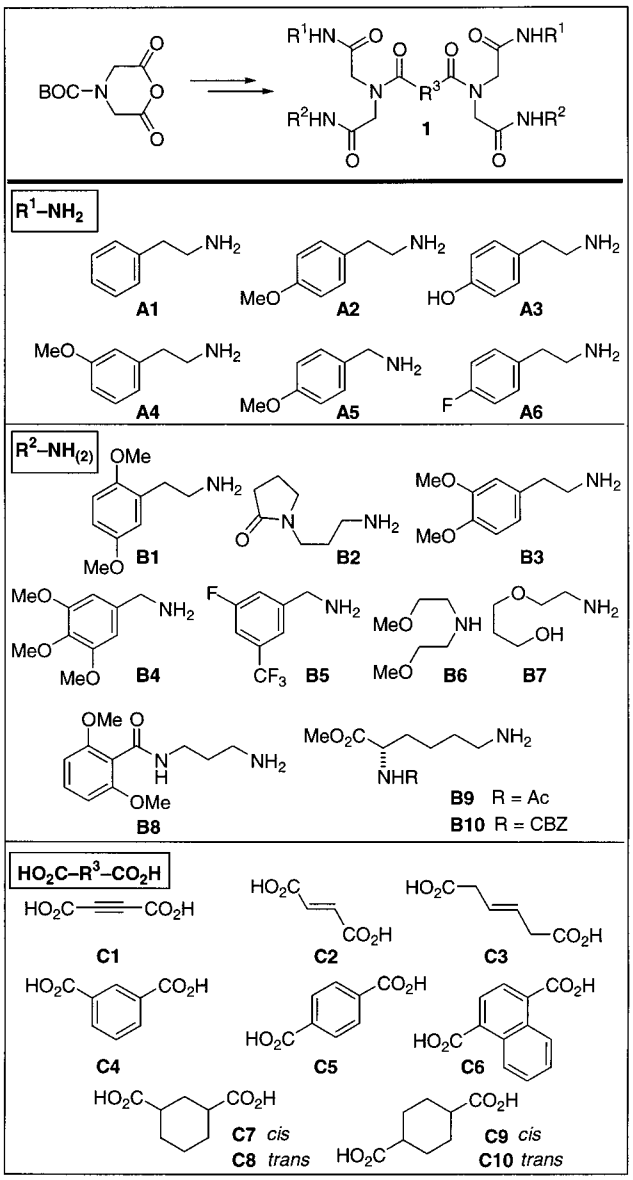

Figure 3. The structure of mixture library **1**. The library was synthesized and screened as mixtures containing single R^1 (**A1**−**A6**) and R^2 (**B1**−**B10**) substitutions, linked by an equimolar mixture of subunit R^3 (**C1**−**C10**): 60 mixtures of 10 compounds, see ref 15.

six different R^1 amines with 10 different R^2 amines through an iminodiacetic acid linker. Each of these combinations was dimerized by coupling to a mixture of 10 dicarboxylic acids (R^3) providing 60 mixtures of 10 compounds.[17] The screen was set up to measure the amount of labeled (biotinylated) MMP2 which binds to $\alpha_V\beta_3$ fixed to a 96-well plate in the presence of the library mixtures, using high-throughput ELISA methods.[18] The mixtures were tested at a concentration of 50 μM (5 μM per component) in 5% DMSO−aqueous buffer, and the data are reported as % binding versus control (DMSO) in Figure 4.[19] Mixtures containing the *N*-α-CBZ-lysine methyl ester (**B10**) subunit were the most effective at inhibiting MMP2 binding, especially in combination with the **A6** (4-fluorophenethylamine) group. The six mixtures containing the **B10** subunit were re-screened at lower concentrations (3 and 10 μM), and again the

(17) The synthesis of this library is described in detail in ref 15.
(18) This assay is described in ref 13.
(19) Instances of observed binding >100% were attributed to precipitation due to the poor solubility of some agents at this concentration, and these results were not further investigated.

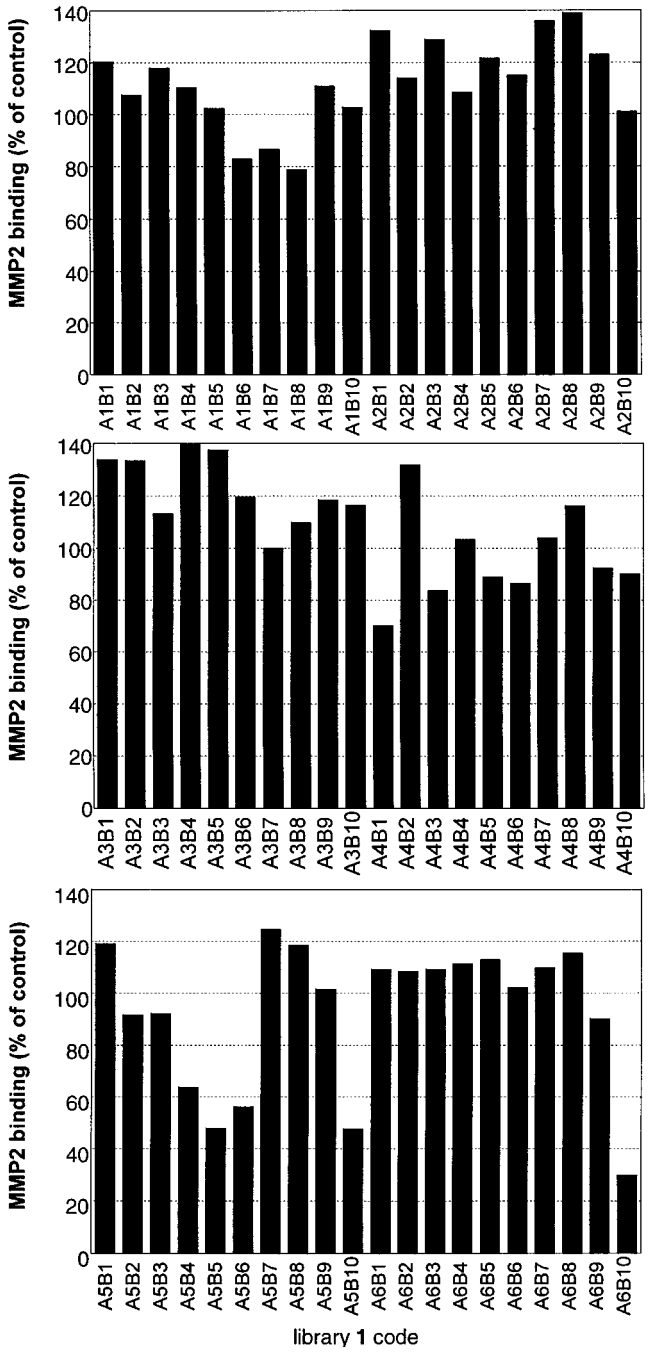

Figure 4. Binding (% of control) of labeled MMP2 to $\alpha_V\beta_3$ in the presence of library **1**. Purified $\alpha_V\beta_3$ was coated onto microtiter plate wells, which were subsequently blocked with casein and incubated (1.5 h, 37 °C) with biotinylated MMP2 (5 nM) and the library components (50 μM mixture concentration, 5% DMSO in the testing media). After removal of unbound enzyme, specific protein binding was quantified by measuring the activity of an HRP-linked antibiotin antibody as described in ref 13. Each **A** and **B** combination is linked by a mixture of 10 dicarboxylic acids, **C1**−**C10**, see Figure 3. Shorter bars (lower MMP2 binding) represent higher inhibitory activity. Observed binding >100% is attributed to the insolubility of some library members.

A6B10 combination was effective. The **A1B10** and **A2B10** mixtures also showed good activity in this concentration range (Figure 5). The 30 individual components making up these three mixtures were prepared and screened in the binding assay at 3 μM. The data for the **A6B10** series are presented in Figure 5. The results revealed that the specific substitution on the benzene ring in the R^1 binding groups (**A1**, **A2**, or **A6**) and the exact

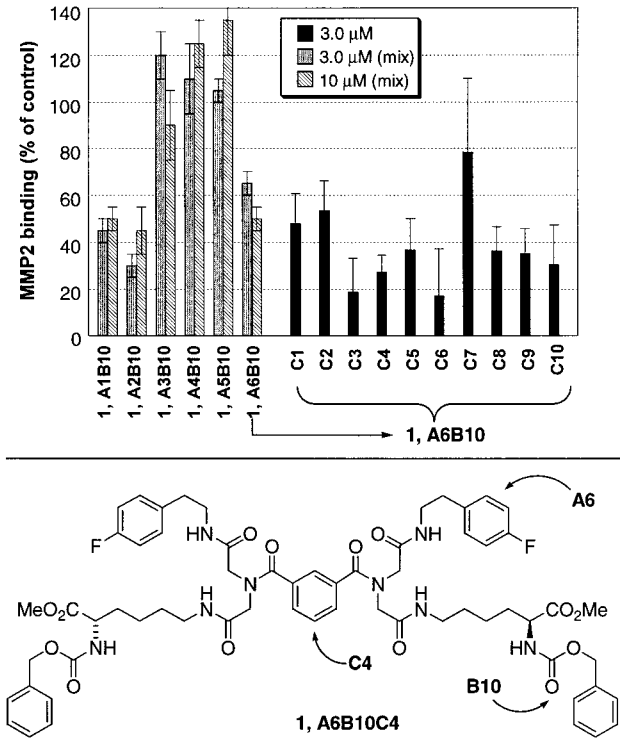

Figure 5. Inhibition of binding by mixtures from library **1** containing the **B10** subunits, and the inhibitory activity of individual compounds from the deconvolution of the **A6B10** mixture. Assays were performed in triplicate as described for Figure 4; bars are the mean ± standard error. Compound **1**, **A6B10C4** was identified as a lead structure for further investigation.

nature of the linking dicarboxylic acid (R^3) were not paramount to the observed reduction in MMP2 binding, implying that the **B10** substitution as the R^2 subunit was key to the antagonist activity. Despite the greater tolerance for variation in the R^1 and R^3 substituents, it was observed that the **A6** substitution (4-fluorophenethylamine) led to the best activity and that the **C4** linker (isophthalic acid) was a good choice for future studies since it was one of the best R^3 substitutions in the **A6B10** series and was active in combination with the other R^1 groups (**A1** and **A2**, data not shown).

A series of **1**, **A6B10C4** analogues were prepared (77 individual compounds) on the basis of the library **1** template, which contain variations in the *N*-α-CBZ-lysine methyl ester (**B10**) subunit.[20] All were screened in the binding assay, and 25 key analogues were identified as having interesting activity and examined more closely (Figures 6 and 7). Of these, the 4-(trifluoromethyl)benzyl carbamate analogue **19** was observed to be the most active, providing concentration-dependent inhibition of MMP2 binding. Notably **19** at 3 μM was more effective than cold MMP2 (200×, 1 μM) at disrupting the labeled MMP2−$\alpha_V\beta_3$ binding and roughly 50% as effective at the equimolar concentration of 1 μM, indicating that **19** is quite effective as disrupting this protein−protein interaction (Figure 7). In addition, analysis of the **B10** analogues in this series provides insight into the functionality required and further modifications that could be expected to be tolerated. Significant changes to the methyl ester group are generally acceptable, and the primary carboxamide **6** is just as active in the binding assay as **1**, **A6B10C4**. Interestingly, analogue **25** which lacks the ester substitution altogether, maintains moderate activity, but compound **23**, the enantiomer of **1**, **A6B10C4**, loses all activity. These results suggested that certain ester or other substitutions at the lysine carboxylate may influence binding but are not key to the observed activity and that this site could be modified in subsequent analogues. Comparisons of **9**−**22** provide information on the impact of modifications to the lysine α-amino group. Benzoyl amide **9** was inactive in the binding assay and was selected as a negative control in subsequent studies (see below). Urea and sulfonamide analogues (**12** and **14**) were less effective than **1**, **A6B10C4**. Analogues **15**, **16**, and **22** have diminished activity, but the other carbamates display equivalent or improved activity, most notably the electron poor benzyl carbamate derivative **19**. The importance of the chain length which

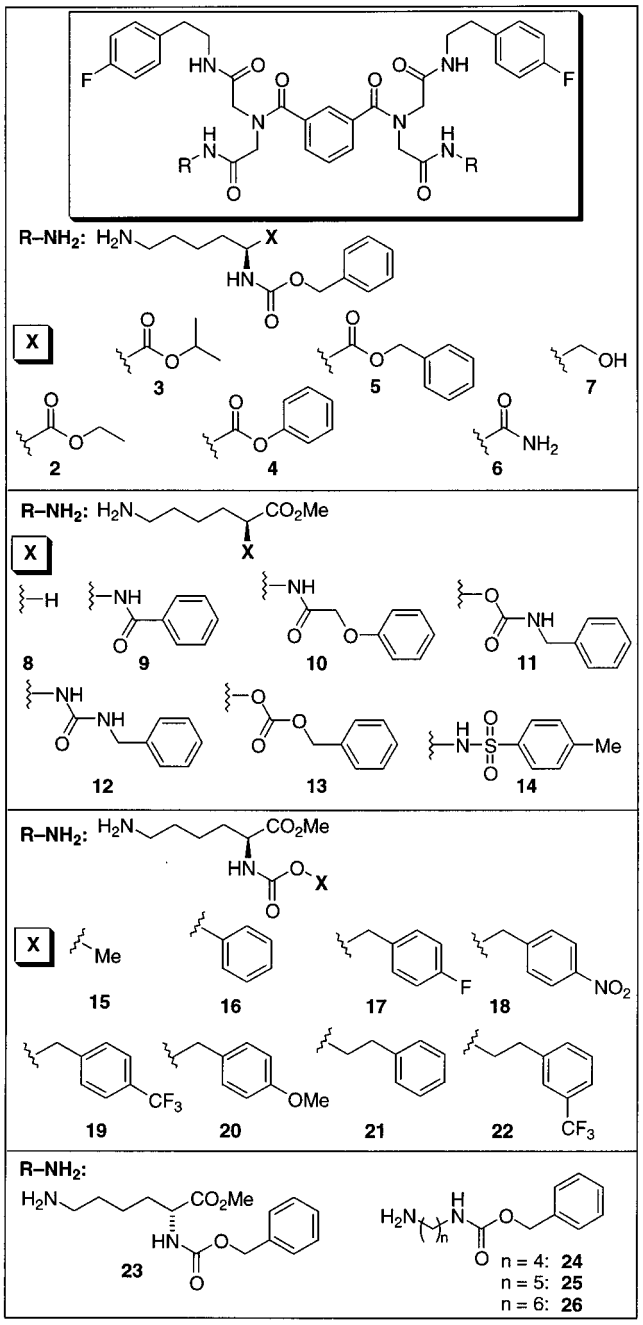

Figure 6. Structures of key **1**, **A6B10C4** analogues screened to improve binding activity. Each analogue contains the 4-fluorophenethylamine (**A6**) subunit in position R^1 and the isophthalic acid (**C4**) linker in position R^3, with modifications to **B10** in position R^2. The structures of the full set (77) of compounds may be found in Supporting Information.

(20) The structures of the complete set of library members are provided in Supporting Information.

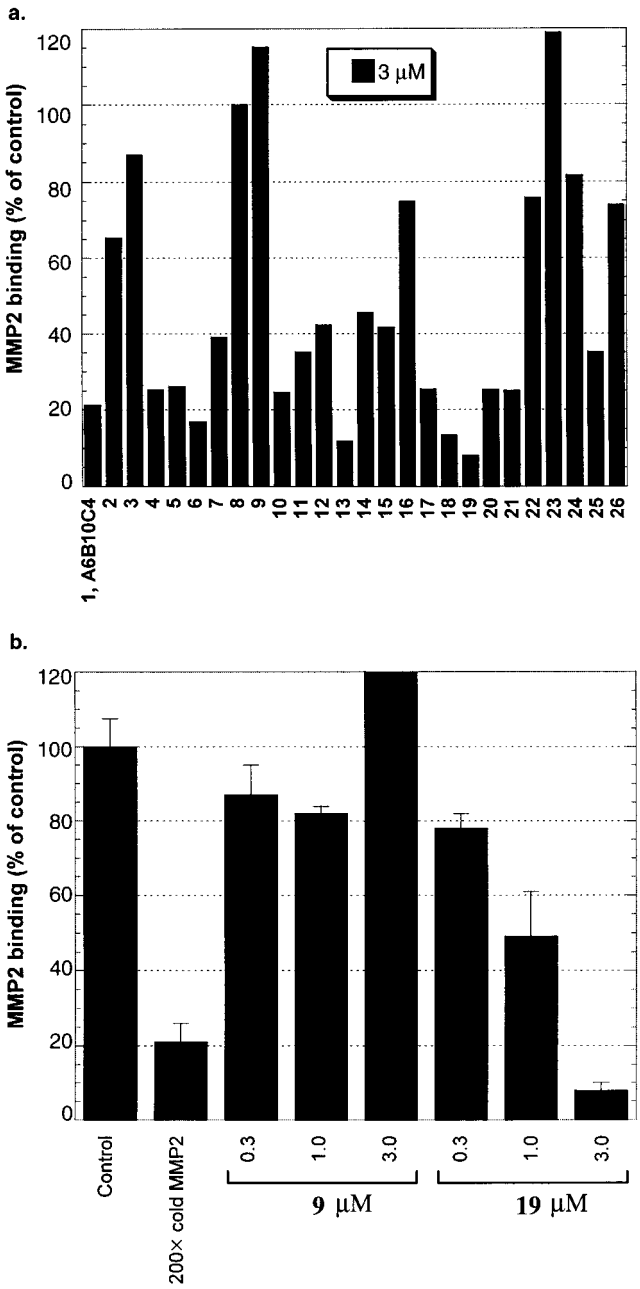

Figure 7. (a) Inhibition of MMP2 binding in the presence of **1**, **A6B10C4** and analogues **2**−**26**. Assays were performed as described for Figure 4. (b) Compound **19** was identified as the most potent agent which displays concentration-dependent inhibition of binding. Compound **9** was selected as a control compound since it displays no significant inhibitory activity despite its overall structural similarity.

separates the carbamate from the molecule core can be inferred from analogues **24**−**26**, where a spacing of 5 methylene units (**25**), as with CBZ-Lys, provides greater activity than the shortened (**24**) or extended (**26**) analogues.

Synthesis of 19 and Derivatives. Having identified **19** as the most potent agent derived from the library screening, the compound was resynthesized to allow more detailed evaluation of its biological properties. A series of additional analogues and partial structures based on **19** were also prepared which defined the functionality necessary for antagonist activity.

Compound **19** was prepared in three steps starting with commercially available *N*-ϵ-BOC-L-lysine methyl ester (Scheme 1). The carbamate was installed in 99% yield by reaction of 4-(trifluoromethyl)benzyl alcohol with *N*,*N*′-disuccinimidyl

Scheme 1

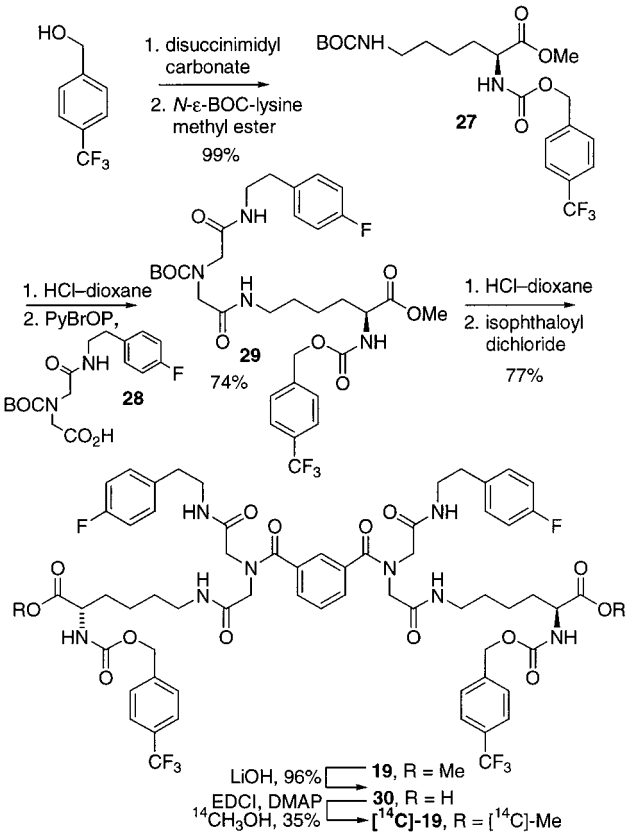

carbonate and subsequent addition to L-Lys(NHBOC)-OCH_3, providing **27**. *N*-BOC deprotection (HCl) and coupling (PyBrOP, 74%) to **28**[15] provided **29**. *N*-BOC deptrotection (HCl) and dimerization upon reaction with isophthaloyl dichloride completed the synthesis and provided **19**. A radiolabel was incorporated by saponification of the two methyl esters (LiOH, 96%) followed by esterification of the resulting dicarboxylic acid **30** with [^{14}C]-methanol mediated by 1-(3-(dimethylamino)-propyl)-3-ethylcarbodiimide hydrochloride (EDCI) and catalytic 4-(dimethylamino)pyridine (DMAP) in 35% yield.

A series of compounds was prepared which lacked the R^1 subunit present in the library compounds (Scheme 2), and these proved key to defining the structural features of **19** contributing to its activity. This was achieved by coupling **27** to *N*-BOC-Gly (EDCI, 96%), providing **31**. *N*-BOC deprotection (HCl) provided the free amine (**32**, 99%), which was dimerized by reaction with isophthaloyl dichloride, providing **33** in 68% yield. The corresponding dicarboxylic acid (**34**) was prepared by saponification of the two methyl esters (LiOH, 93%). A radiolabel was incorporated into compound **34** by repeating its synthesis utilizing *N*-BOC-[1-^{14}C]-Gly. Smaller substructure analogues of **19** were prepared by reacting intermediate **32** with benzoyl chloride (90%), providing **35**. Carboxylic acid **36** was prepared by treatment of **35** with LiOH in 88% yield. An additional substructure analogue with functionality designed to increase aqueous solubility was prepared by coupling **32** with diglycolic acid, resulting in carboxylic acid **37** in 77% yield.

Similar modifications to the inactive control compound **9** were made for study where the 4-fluorophenethylamine subunit was omitted and the methyl esters on the lysine portion were hydrolyzed to improve aqueous solubility (Scheme 3). The synthesis was achieved by reacting the free amine of *N*-ϵ-BOC-lysine methyl ester with benzoyl chloride, providing benzoyl amide **38** in 78% yield. The *N*-BOC protecting group was

Scheme 2

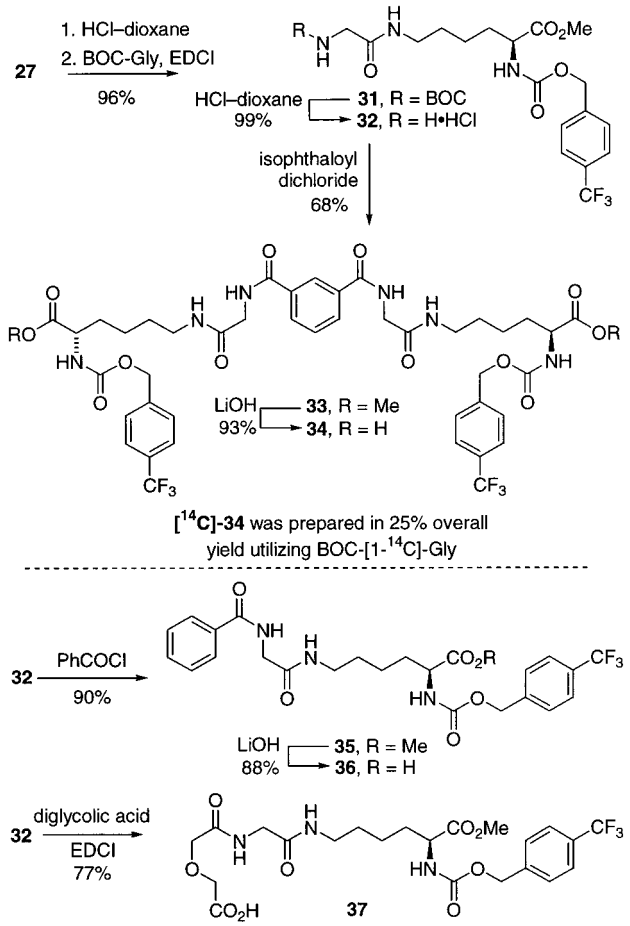

Scheme 3

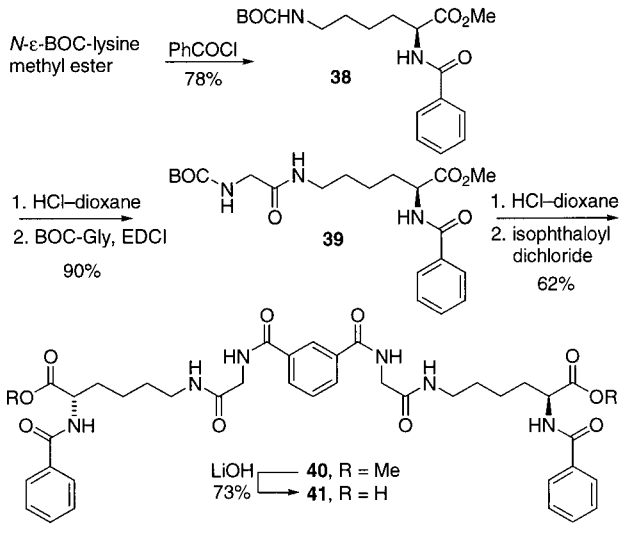

cleaved (HCl) and the resulting free amine coupled to *N*-BOC-Gly (EDCI, 90%). After deprotection, this diamide (**39**) was dimerized by reaction with isophthaloyl dichloride, providing dimethyl ester **40** (62%). Dicarboxylic acid **41** was prepared by saponification of the two lysine methyl esters (LiOH, 73%).

Biological Properties of 19 and Derivatives. Compound **19** was examined in detail to determine its target protein and to define its biological properties. Benzoyl amide **9** was selected as a negative control compound since it was found to lack antagonist activity in the binding assay, despite its similar overall structure and physical properties (e.g., solubility and hydrophobicity). After incubation (at 3 μM) with fixed $\alpha_V\beta_3$ and removal of unbound compound, **[^{14}C]-19** was found to adhere to the integrin, as measured by the radioactivity (CPMs) retained on the protein (Figure 8). Incubation in the presence of a 25-fold molar excess of cold **19** significantly reduced the amount of bound agent, whereas incubation in the presence of a 25-fold molar excess of (cold) control compound **9** did not affect the binding of **[^{14}C]-19**. In a similar experiment measuring the interaction of **[^{14}C]-19** to fixed MMP2 (Figure 9), no significant binding was observed. These results indicate that the antagonist activity observed in the MMP2−$\alpha_V\beta_3$ binding assay is derived from the binding of **19** to $\alpha_V\beta_3$. The nature of the **19**−$\alpha_V\beta_3$ interaction was shown to be independent of the integrin site that recognizes the Arg-Gly-Asp sequence, as the high-affinity cyclic RGD peptide *cyclo*(Arg-Gly-Asp-D-Phe-Val)[21] did not compete for **[^{14}C]-19** binding (Figure 8). Moreover **19** did not inhibit the binding of vitronectin to $\alpha_V\beta_3$, further indicating that the binding site for **19** is distinct from that which binds RGD-ligands (Figure 10). In an assay which measures the ability of purified MMP2 to degrade a [^{3}H]-collagen-IV matrix, compound

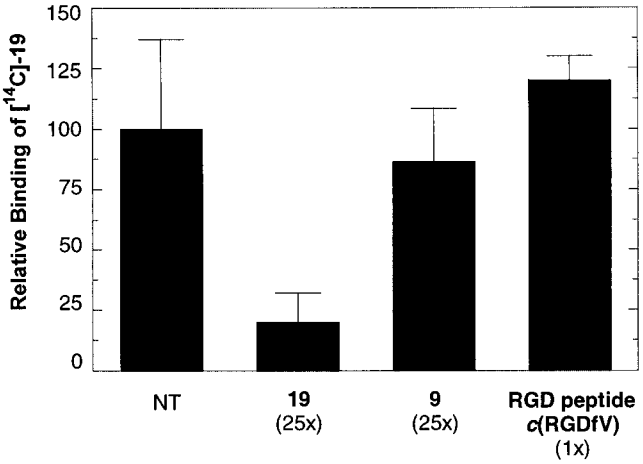

Figure 8. ^{14}C-labeled **19** binds specifically to $\alpha_V\beta_3$. Purified $\alpha_V\beta_3$ (10 μg/mL) was plated onto microtiter plate wells overnight at 4 °C prior to blocking with casein and incubation with **[^{14}C]-19** (3 μM). Bound agent was competed off the integrin by a 25-fold molar excess of cold **19**, but not **9** or the RGD-peptide *c*(RGDfV). See text for details.

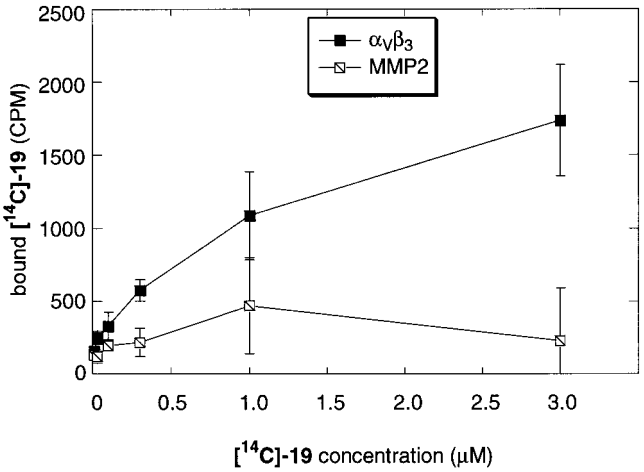

Figure 9. **[^{14}C]-19** binds integrin $\alpha_V\beta_3$ but has no significant binding to MMP2 in the same concentration range. Purified proteins were coated onto microtiter plates prior to blocking with casein and incubation with **[^{14}C]-19**.

(21) Haubner, R.; Gratias, R.; Diefenbach, B.; Goodman, S. L.; Jonczyk, A.; Kessler, H. *J. Am. Chem. Soc.* **1996**, *118*, 7461.

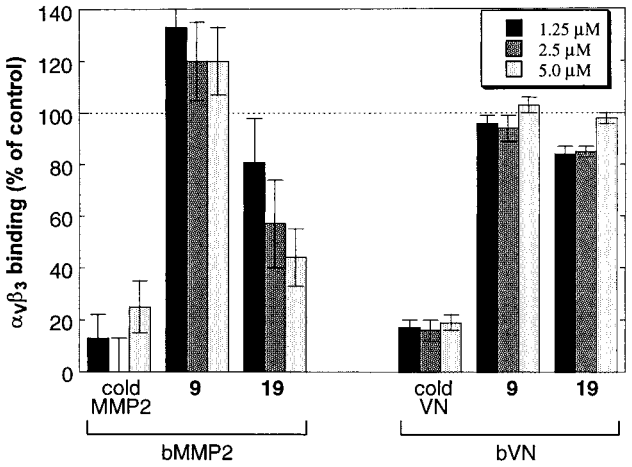

Figure 10. Binding of biotinylated MMP2 (left) and vitronectin (VN) (right) to integrin $\alpha_V\beta_3$. Compound **19** disrupts the binding of MMP2 but does not affect the binding of the integrin's endogenous ligand, vitronectin, which recognizes $\alpha_V\beta_3$ through its RGD sequence. Compound **9** has no significant inhibitory effect for either protein−protein interaction. Purified $\alpha_V\beta_3$ (10 μg/mL, 50 μL/well) was coated onto microtiter plates and incubated with biotinylated MMP2 and VN in the presence of **9** and **19**. Protein binding was assessed by measuring the activity of an HRP-conjugated antibiotin antibody, followed by color development using TMB peroxidase substrate.

19 (at 3 μM) did not have an effect on the enzyme's proteolytic activity. This indicates that, at concentrations where binding inhibition was observed, **19** does not function as a direct enzyme inhibitor.

These experiments support the expectation that compound **19** may disrupt the ability of tumor cells to utilize MMP2 to degrade ECM proteins in a manner analogous to that of PEX. This agent does not interfere with the binding of $\alpha_V\beta_3$ to its classical RGD ligands nor does it function as a direct protease inhibitor. Since it is believed that MMP2 binding to $\alpha_V\beta_3$ is necessary for angiogenesis as demonstrated with PEX, the in vivo effects of **19** on bFGF-induced angiogenesis were examined in chick embryo and mouse models. Although preliminary results provided indications of the predicted in vivo activity (data not shown), the experiments were hampered by the poor physical properties of the agent, most notably its low aqueous solubility. Since the primary screen of our libraries indicated that not all of the functionality of **19** was necessary and that there were sites on the molecule that could be modified to improve its properties, we examined a series of substructure analogues and derivatives of **19** (see Schemes 1−3) that had better solubility characteristics in search of an agent more suited for in vivo testing.

Lysine derivative **27**, the simplest substructure of **19**, was found to display no measurable inhibition in the MMP2−$\alpha_V\beta_3$ binding assay, nor did the monomeric iminodiacetic diamide **29** (Figure 11). Some inhibition was observed with **33** at low concentrations; however at higher concentrations it appeared to suffer from poor solubility. Since **33** comprises dimerized product **19** without the R^1 (4-fluorophenethylamine) subunit, its activity further demonstrates that this portion of the molecule may not be required for biological activity. Amide **35** was almost as effective as **19**, despite consisting of only a portion of the dimerized structure (Figure 11). These results indicated that the R^1 subunit or a dimerized product displaying two identical binding groups may not be necessary.

Results for an important set of substructures which contain further modifications designed to increase aqueous solubility

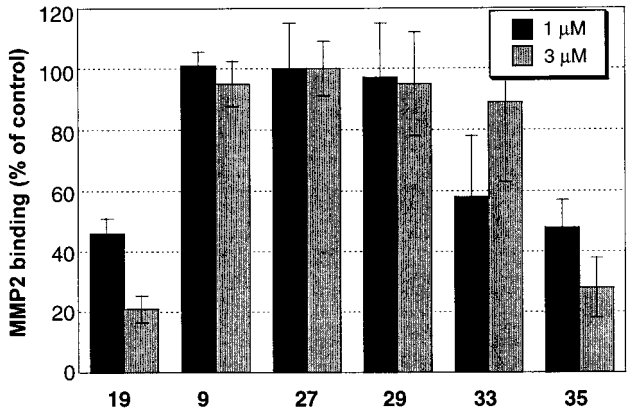

Figure 11. Inhibition of MMP2 binding to $\alpha_V\beta_3$ by partial structures **27**, **29**, **33**, and **35** (see Schemes 1 and 2 for structures). The assay was performed in triplicate as described for Figure 4; bars are the mean ± standard error.

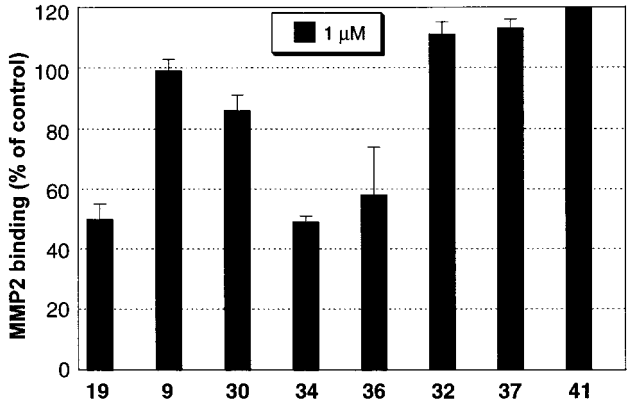

Figure 12. Inhibition of MMP2 binding to $\alpha_V\beta_3$ by water-soluble derivatives **30**, **32**, **34**, **36**, **37**, and **41** (see Schemes 1−3 for structures). The assay was performed in triplicate as described for Figure 4; bars are the mean ± standard error. Compound **34** was identified as having comparable inhibitory activity to that of compound **19**.

are shown in Figure 12. Compounds **32** and **37**, which lack the benzoyl (or isophthaloyl) amides present in all previously active agents, displayed no inhibition. Dicarboxylic acid **30**, however, had some activity, consistent with previously studied analogues which indicated that the ester was not necessary for binding. Substructure **34**, the dicarboxylic acid derivative of **33**, was found to effectively inhibit MMP2 binding at a level similar to **19**, despite lacking the R^1 (4-fluorphenethylamine, **A6**) and methyl ester substituents. Monocarboxylic acid **36** also appeared to have moderate activity in the binding assay, although its activity was weak and variable in subsequent studies. Compound **41**, a water-soluble derivative of control compound **9**, was similarly found to lack antagonist activity in the binding assay and was thus selected to serve as a control for subsequent experiments.

Compound **34** was selected for detailed study and was found to have activity comparable to **19** in all the additional in vitro assays described above. Thus, it was shown to bind $\alpha_V\beta_3$, but not MMP2, in a dose-dependent manner and it did not inhibit the binding of vitronectin to $\alpha_V\beta_3$. It also displayed minimal interaction with integrin $\alpha_5\beta_1$, which does not recognize MMP2. The $\alpha_V\beta_3$ binding of **[^{14}C]-34** is inhibited with cold **34** but not control compound **41**. Compound **34** was further found to block the ability of $\alpha_V\beta_3$-transfected melanoma cells to utilize MMP2 and degrade a collagen IV matrix in a β_3-dependent manner, and as was observed with **19**, it had no direct inhibitory effect on purified MMP2 catalytic activity. Compound **34** also

possesses a number of features which made it more suited for in vivo testing, including better aqueous solubility, a lower molecular weight, and the lack of labile functionality (i.e., the methyl ester). Full details of the in vitro properties as well as in vivo biological activity of **34** and **[^{14}C]-34** are described elsewhere.[22] Importantly, it was found to be a potent inhibitor of angiogenesis in a chick CAM model and led to the near complete reduction of the growth of solid tumors in vivo, validating this new target and representing a rare example of a small molecule therapeutic intervention through disruption of a specific protein−protein interaction.[23,24]

Experimental Section

(*S*)-Methyl 6-(((*tert*-Butyloxy)carbonyl)amnio)-2-((4-trifluoromethyl)benzyloxycarbonyl)hexanoate (27). A solution of *N*,*N*′-disuccinimidyl carbonate (5.38 g, 21 mmol) in acetonitrile (150 mL) was treated with 4-(trifluoromethyl)benzyl alcohol (2.87 mL, 21 mmol) and Et_3N (5.8 mL, 42 mmol) and stirred at 25 °C. After 3 h, the reaction mixture was added to a flask containing *N*-ϵ-BOC-lysine methyl ester (4.2 g, 14 mmol) in acetonitrile and stirred for an additional 3 h. The solvent was evaporated and the residue dissolved in CH_2Cl_2 (250 mL) and washed with 10% aqueous HCl (2 × 200 mL) and saturated aqueous $NaHCO_3$ (200 mL). Flash chromatography (SiO_2, 3:1 CH_2Cl_2/EtOAc) provided 6.4 g (99%) of **27** as a pale yellow oil: $[\alpha]^{25}_D$ −8.9 (*c* 5.6, CH_3OH); ^{1}H NMR ($CDCl_3$, 400 MHz) δ 7.57 (d, J = 8.1 Hz, 2H), 7.39 (d, J = 8.1 Hz, 2H), 5.70 (d, J = 7.9 Hz, 1H), 5.13 (m, 2H), 4.71 (m, 1H), 4.28 (m, 1H), 3.67 (s, 3H), 3.03 (m, 2H), 1.78 (m, 1H), 1.64, (m, 1H) 1.46−1.32 (m, 4H) 1.35 (s, 9H); ^{13}C NMR ($CDCl_3$, 100 MHz) δ 172.9, 156.2, 155.8, 140.4, 130.1 (q, J = 32.0 Hz), 127.8, 125.3, 122.9 (q, J = 270.0 Hz), 79.1, 65.8, 53.7, 52.3, 39.8, 31.7, 29.5, 28.4, 22.2; IR (film) ν_{max} 3357, 2952, 1790, 1745, 1524 cm^{-1}; FABHRMS (NBA-NaI) *m*/*z* 463.2044 (M + H$^+$, $C_{21}H_{29}F_3N_2O_6$ requires 463.2056).

(*S*)-*N*-((*tert*-Butyloxy)carbonyl)-*N*′-((4-fluorophenyl)ethyl)-*N*″-(5-methoxycarbonyl)-5-(4-(trifluoromethyl)benzyloxycarbonyl)amino)-pentyl)iminodiacetic Acid Diamide (29). A solution of **27** (2.2 g, 4.8 mmol) in CH_2Cl_2 (3 mL) was treated with 4 N HCl−dioxane (10 mL) and stirred for 20 min at 25 °C. Solvent and excess acid were removed under reduced pressure, and the crude hydrochloride salt was dissolved in DMF (40 mL), treated with *N*-((*tert*-butyloxy)carbonyl)-*N*′-(2-(4-fluorophenyl)ethyl)iminodiacetic acid monoamide[15] (**28**, 1.68 g, 4.8 mmol), PyBrOP (3.3 g, 7.1 mmol), and *i*-Pr_2NEt (5.0 mL, 29 mmol), and stirred for 1 h at 25 °C. The reaction mixture was diluted with EtOAc (400 mL) and washed with 10% aqueous HCl (2 × 300 mL) and saturated aqueous $NaHCO_3$ (300 mL). Flash chromatography (SiO_2, 1:1 CH_2Cl_2/EtOAc) provided 2.47 g (74%) of **29** as a white foamy solid: $[\alpha]^{25}_D$ −7.1 (*c* 4.5, CH_3OH); ^{1}H NMR ($CDCl_3$, 400 MHz) δ 8.23 and 7.59 (two m, 1H), 7.58 (d, J = 8.1 Hz, 2H), 7.43 (m, 2H), 7.13 (m, 2H), 7.06 and 6.78 (two m, 1H), 6.94 (m, 2H), 5.70 (dd, J = 12.9 and 8.2 Hz, 1H), 5.11 (m, 2H), 4.31 (m, 1H), 3.85−3.72 (m, 4H), 3.71 (s, 3H), 3.49 (m, 2H), 3.22 (m, 2H), 2.79 (m, 2H), 1.81−1.39 (m, 6H) 1.38 (s, 9H); ^{13}C NMR ($CDCl_3$, 100 MHz) δ 172.8, 170.0, 169.9, 155.8, 154.8, 161.4 (d, J = 242.7 Hz), 140.2, 134.4, 130.1 (q, J = 33.4 Hz), 130.0, 127.7, 125.3 (q, J = 3.0 Hz), 123.8 (q, J = 299.9 Hz), 115.0, 81.2, 65.7, 53.9, 53.8, 53.3, 52.2, 40.8, 38.6, 34.4, 31.5, 28.4, 28.0, 22.4; IR (film) ν_{max} 3267, 2935, 1708, 1657, 1511 cm^{-1}; FABHRMS (NBA-CsI) *m*/*z* 831.2026 (M + Cs$^+$, $C_{33}H_{42}F_4N_4O_8$ requires 831.1993).

***N*,*N*′-Bis-[(2-[4-fluorophenyl]ethyl)carboxamidomethyl]-*N*,*N*′-bis-[*N*-(5-(*S*)-(methoxycarbonyl)-5-[((4-trifluoromethyl)benzyloxycarbonyl)amino]pentyl)carboxamidomethyl]benzene-1,3-dicarboxamide (19).** A solution of **29** (2.10 g, 3.0 mmol) in CH_2Cl_2 (5 mL) was treated with 4 N HCl−dioxane (10 mL) and stirred for 0.5 h at 25 °C. Solvent and excess acid were removed under reduced pressure, and the crude hydrochloride salt was suspended in CH_2Cl_2 (30 mL), treated with isophthaloyl dichloride (305 mg, 1.5 mmol) and *i*-Pr_2NEt (1.04 mL, 6.0 mmol), and stirred for 4 h at 25 °C. The reaction mixture was diluted with EtOAc (500 mL) and washed with 10% aqueous HCl (2 × 300 mL) and 5% aqueous Na_2CO_3 (300 mL), dried (Na_2SO_4), and evaporated. Flash chromatography (SiO_2, 1:4.5:4.5 MeOH/CH_2Cl_2/EtOAc) provided 1.54 g (77%) of **19** as a white powder: $[\alpha]^{25}_D$ −5.5 (*c* 2.8, CH_3OH); ^{1}H NMR (CD_3OD, 400 MHz) δ 7.62 (m, 4H), 7.52 (m, 4H), 7.42 (m, 4H), 7.19 (m, 4H), 6.96 (m, 4H), 5.14 (m, 4H), 4.16 (m, 2H), 4.13 (m, 2H), 4.08 (m, 2H), 3.99 (m, 4H), 3.68 (s, 6H), 3.45−3.35 (m, 4H), 3.25−3.11 (m, 4H), 2.82−2.70 (m, 4H), 1.82 (m, 2H), 1.69 (m, 2H) 1.60−1.34 (m, 8H); ^{13}C NMR (CD_3OD, 100 MHz) δ 174.5, 173.4, 171.1, 170.8, 169.9 (d, J = 241.1 Hz), 158.2, 142.7, 136.8, 136.2, 131.5, 130.8 (q, J = 31.8 Hz), 130.0, 129.5, 128.9, 128.8, 126.3, 125.6 (q, J = 268.7 Hz), 116.0 (d, J = 20.2 Hz), 66.5, 55.4, 55.3, 53.0, 52.7, 42.0, 40.1, 35.5, 32.0, 29.7, 24.2; IR (film) ν_{max} 3291, 2936, 1725, 1651, 1326 cm^{-1}; FABHRMS (NBA-CsI) *m*/*z* 1459.4015 (M + Cs$^+$, $C_{64}H_{70}F_8N_8O_{14}$ requires 1459.3938).

***N*,*N*′-Bis-[(2-[4-fluorophenyl]ethyl)carboxamidomethyl]-*N*,*N*′-bis-[*N*-(5-(*S*)-carboxy-5-[((4-trifluoromethyl)benzyloxycarbonyl)amino]-pentyl)carboxamidomethyl]benzene-1,3-dicarboxamide (30).** A solution of **19** (100 mg, 0.075 mmol) in THF−MeOH (0.8 mL, 1:1) was treated with LiOH·H_2O (12.6 mg, 0.30 mmol) dissolved in H_2O (0.2 mL) and stirred for 2 h at 0 °C. The reaction mixture was quenched by the addition of 10% aqueous HCl (10 mL) and extracted with EtOAc (3 × 10 mL). The combined organic layers were washed with saturated aqueous NaCl (10 mL), dried (Na_2SO_4), and evaporated to afford 95 mg (96%) of **30** as a white powder: $[\alpha]^{25}_D$ +0.8 (*c* 5.0, CH_3OH); ^{1}H NMR (DMSO-d_6, 400 MHz) δ 12.54 (br s, 2H), 8.63 (m, 1H), 8.43 (m, 2H), 8.30 (m, 1H), 7.74 (m, 4H), 7.69 (m, 2H), 7.57 (m, 4H), 7.40 (m, 4H), 7.24 (m, 4H), 7.09 (m, 4H), 5.15 (m, 4H), 4.14 (m, 2H), 4.02−3.87 (m, 8H), 3.31 (m, 4H), 3.208 (m, 4H), 2.74 (m, 4H), 1.71 (m, 2H), 1.62 (m, 2H) 1.50−1.34 (m, 8H); ^{13}C NMR (CD_3OD, 100 MHz) δ 175.8, 173.5, 171.1, 170.8, 162.9 (d, J = 241.2 Hz), 158.3, 142.8, 136.8, 136.2, 131.5, 130.8 (q, J = 32.0 Hz), 130.1, 129.6, 128.8, 126.3, 125.6 (q, J = 270.1 Hz), 116.1 (d, J = 21.7 Hz), 66.5, 55.3, 55.2, 53.0, 42.0, 40.1, 35.3, 32.1, 29.7, 24.3; IR (film) ν_{max} 3287, 2928, 1705, 1659, 1320 cm^{-1}; MALDIFTMS *m*/*z* 1321.4493 (M + Na$^+$, $C_{62}H_{66}F_8N_8O_{14}$ requires 1321.4468).

[^{14}C]-19. A suspension of **30** (1.7 mg, 1.3 μmol) and EDCI (2.0 mg, 10.3 μmol) in DMF (20 μL) was treated with a solution of $^{14}CH_3OH$ (American Radiolabeled Chemicals, 0.3 mCi, 57 mCi/mmol, 5.2 μmol) in CH_2Cl_2 (0.3 mL) and a solution of DMAP (73 μg, 0.6 μmol) in CH_2Cl_2 (35 μL) and stirred for 4 h at 0 °C. The reaction mixture was diluted with EtOAc (3 mL), washed with 10% aqueous HCl (3 × 3 mL) and saturated aqueous $NaHCO_3$ (3 mL), and dried (Na_2SO_4). PTLC (SiO_2, 2:3:3 EtOH/$CHCl_3$/EtOAc) provided 0.6 mg (35%) of **[^{14}C]-19** as a white film. This material was identical to the corresponding unlabeled dimethyl ester (**19**) by ^{1}H NMR and TLC. The relative activity was approximately 104 mCi/mmol.

(*S*)-Methyl 6-[2-(((*tert*-Butyloxy)carbonyl)amino)acetamido]-2-[(4-trifluoromethyl)benzyloxycarbonyl]hexanoate (31). A solution of **27** (2.7 g, 5.8 mmol) in CH_2Cl_2 (3 mL) was treated with 4 N HCl−dioxane (10 mL) and stirred for 20 min at 25 °C. Solvent and excess acid were removed under reduced pressure, and the crude hydrochloride salt was dissolved in DMF (50 mL), treated with *N*-BOC-Gly (1.0 g, 5.8 mmol), EDCI (1.2 g, 6.4 mmol), and *i*-Pr_2NEt (2.0 mL, 11.6 mmol), and stirred for 12 h at 25 °C. The reaction mixture was diluted with EtOAc (400 mL) and washed with 10% aqueous HCl (3 × 250 mL) and saturated aqueous $NaHCO_3$ (250 mL), dried (Na_2SO_4), and evaporated to provide 2.89 g (96%) of **31** as a white foamy solid: $[\alpha]^{25}_D$ −10.4 (*c* 2.5, CH_3OH); ^{1}H NMR ($CDCl_3$, 400 MHz) δ 7.59 (m, 2H), 7.45 (m, 2H), 6.19 (m, 1H), 5.51 (m, 1H), 5.13 (m, 2H), 4.32 (m, 2H), 3.74 (s, 3H), 3.73 (m, 2H), 3.26 (m, 2H), 1.81−1.39 (m, 6H) 1.44 (s, 9H); ^{13}C NMR (CD_3OD, 100 MHz) δ 174.5, 172.2, 158.2, 158.1, 142.7, 130.8 (q, J = 31.8 Hz), 128.8, 126.3, 125.5 (q, J = 269.7 Hz), 80.5, 66.5, 55.3, 52.7, 44.6, 39.8, 32.1, 29.8, 28.6, 24.0; IR (film) ν_{max} 3320, 2932, 1721, 1692, 1326 cm^{-1}; FABHRMS (NBA-CsI) *m*/*z* 652.1234 (M + Cs$^+$, $C_{23}H_{32}F_3N_3O_7$ requires 652.1247).

(*S*)-Methyl 6-[2-(Amino)acetamido]-2-[(4-trifluoromethyl)benzyloxycarbonyl]hexanoate Hydrochloride (32). A solution of **31** (350

(22) Silletti, S.; Kessler, T.; Goldberg, J.; Boger, D. L.; Cheresh, D. A. *Proc. Natl. Acad. Sci. U.S.A.* **2001**, *98*, 119.

(23) Cochran, A. G. *Chem. Biol.* **2000**, *7*, R85.

(24) In vitro cytotoxic activity (L1210 IC_{50}) of key structures: **19**, 6 μM; **34**, 45 μM; **9**, 70 μM; **41**, >100 μM (34% inhibition at 100 μM).

mg, 0.67 mmol) in CH_2Cl_2 (2 mL) was treated with 4 N HCl−dioxane (5.0 mL) and stirred at 25 °C. After 0.5 h, solvent and excess acid were removed under reduced pressure, providing 300 mg (99%) of **31** as a pale yellow oil: $[\alpha]^{25}_D$ −10.4 (*c* 3.0, CH_3OH); ^{1}H NMR (CD_3OD, 400 MHz) δ 7.65 (d, J = 8.2 Hz, 2H), 7.48 (d, J = 8.2 Hz, 2H), 5.18 (d, J = 13.3 Hz, 1H), 5.16 (d, J = 13.3 Hz, 1H), 4.16 (m, 1H), 3.70 (s, 3H), 3.65 (s, 2H), 3.21 (t, J = 7.1 Hz, 2H), 1.84 (m, 1H), 1.68 (m, 1H), 1.54 (m, 2H), 1.42 (m, 2H); ^{13}C NMR (CD_3OD, 100 MHz) δ 174.5, 167.1, 158.2, 142.8, 130.8 (q, J = 31.8 Hz), 128.8, 126.3, 125.5 (q, J = 270.1 Hz), 66.5, 55.4, 52.7, 41.5, 40.2, 32.1, 29.6, 24.1; IR (film) ν_{max} 3317, 2954, 1718, 1684, 1530, 1327 cm^{-1}; MALDIFTMS (DHB) *m*/*z* 442.1586 (M + Na$^+$, $C_{18}H_{24}F_3N_3O_5$ requires 442.1566).

***N,N′*-Bis-[(5-(*S*)-(methoxycarbonyl)-5-[((4-trifluoromethyl)benzyloxycarbonyl)amino]pentyl)carboxamidomethyl]benzene-1,3-dicarboxamide (33).** A solution of **31** (2.05 g, 4.0 mmol) in CH_2Cl_2 (3.0 mL) was treated with 4 N HCl−dioxane (10.0 mL) and stirred for 20 min at 25 °C. Solvent and excess acid were removed under reduced pressure, and the crude hydrochloride salt was suspended in DMF (40 mL), treated with isophthaloyl dichloride (400 mg, 2.0 mmol) and *i*-Pr_2NEt (1.4 mL, 8.0 mmol), and stirred for 1 h at 25 °C. The reaction mixture was diluted with EtOAc (400 mL) and washed with 10% aqueous HCl (3 × 200 mL) and 5% aqueous Na_2CO_3 (200 mL), dried (Na_2SO_4), and evaporated. Flash chromatography (SiO_2, 1:4.5:4.5 MeOH/CH_2Cl_2/EtOAc) provided 1.30 g (68%) of **33** as a yellow powder: $[\alpha]^{25}_D$ −6.4 (*c* 2.1, CH_3OH); ^{1}H NMR ($CDCl_3$, 400 MHz) δ 8.29 (m, 2H), 8.11 (m, 2H), 7.87 (m, 4H), 7.53 (m, 2H), 7.39 (m, 2H), 6.88 (m, 2H), 5.94 (m, 2H), 5.08 (m, 4H), 4.30 (m, 2H), 4.01 (m, 4H), 3.70 (s, 6H), 3.23 (m, 4H), 1.77 (m, 2H), 1.67 (m, 2H), 1.51 (m, 4H), 1.37 (m, 4H); ^{13}C NMR (CD_3OD, 100 MHz) δ 174.6, 171.5, 169.3, 158.3, 142.7, 135.3, 131.6, 130.8 (q, J = 32.2), 129.8, 128.8, 127.6, 126.3, 125.5 (q, J = 269.2), 66.5, 55.4, 52.7, 44.1, 40.0, 32.1, 29.8, 24.1; IR (film) ν_{max} 3305, 2951, 1716, 1651, 1538 cm^{-1}; FABHRMS (NBA-CsI) *m*/*z* 1101.2398 (M + Cs$^+$, $C_{44}H_{50}F_6N_6O_{12}$ requires 1101.2445).

***N,N′*-Bis[(5-(*S*)-carboxy-5-[((4-trifluoromethyl)benzyloxycarbonyl)-amino]pentyl)carboxamidomethyl]benzene-1,3-dicarboxamide (34).** A solution of **33** (0.95 g. 0.98 mmol) in THF−MeOH (8.0 mL, 3:1) was treated with LiOH·H_2O (165 mg, 3.9 mmol) in H_2O (2.0 mL) and stirred at 0 °C. After 2 h, the reaction was quenched by the addition of 10% aqueous HCl (20 mL) and the mixture was extracted with EtOAc (3 × 50 mL). The organic layers were combined and washed with saturated aqueous NaCl (50 mL), dried (Na_2SO_4), and evaporated to provide 0.86 g (93%) of **34** as a white powder: $[\alpha]^{25}_D$ −0.6 (*c* 3.2, CH_3OH); ^{1}H NMR (CD_3OD, 400 MHz) δ 8.40 (m, 1H), 8.03 (dd, J = 1.8, 7.8 Hz, 2H), 7.62 (d, J = 8.1 Hz, 4H), 7.53 (t, J = 6.1 Hz, 1H), 7.51 (d, J = 8.1 Hz, 4H), 5.16 (d, J = 13.3 Hz, 2H), 5.13 (d, J = 13.3 Hz, 2H), 4.12 (m, 2H), 4.00 (s, 4H), 3.22 (t, J = 6.6 Hz, 4H), 1.85 (m, 2H), 1.70 (m, 2H), 1.55 (m, 4H), 1.37 (m, 4H); ^{13}C NMR (CD_3OD, 100 MHz) δ 175.9, 171.6, 169.4, 158.4, 142.8, 135.4, 131.6, 130.5 (q, J = 31.8), 129.8, 128.8, 127.7, 126.3, 125.6 (q, J = 268.7), 66.5, 53.3, 44.2, 40.1, 32.2, 29.8, 24.2; IR (film) ν_{max} 3334, 2933, 1718, 1646, 1631, 1528 cm^{-1}; MALDIFTMS (DHB) *m*/*z* 963.2953 (M + Na$^+$, $C_{42}H_{46}F_6N_6O_{12}$ requires 963.2976).

[^{14}C]-34. A solution of [1-^{14}C]-glycine (American Radiolabeled Chemicals, 1.0 mCi, 55 mCi/mmol, 0.018 mmol) in 0.1 N HCl was transferred to a 4 mL vial, and the solvent was removed under a stream of N_2. The resulting residue was treated with a solution of $NaHCO_3$ (4.6 mg, 0.054 mmol) in H_2O (0.25 mL) and a solution of di-*tert*-butyl dicarbonate (10.5 μL, 0.045 mmol) in THF (0.25 mL) and stirred at 25 °C. After 12 h the solution had become homogeneous and was diluted with H_2O (1.0 mL) and washed with Et_2O (2 × 1.0 mL). The aqueous solution was acidified by the addition of 10% aqueous HCl (0.5 mL) and extracted with EtOAc (4 × 1.0 mL). The combined extracts were dried (Na_2SO_4) and evaporated under a stream of N_2 to provide 2.9 mg (92%) of [1-^{14}C]-*N*-BOC-glycine as a white film.

A solution of **27** (50 mg, 0.11 mmol) in CH_2Cl_2 (1 mL) was treated with 4 N HCl−dioxane (1 mL) and stirred for 1 h at 25 °C. The reaction mixture was diluted with EtOAc (25 mL) and washed with 10% aqueous Na_2CO_3 (25 mL) and saturated aqueous NaCl (25 mL), dried (Na_2SO_4), and evaporated to provide the deprotected lysine as a colorless film. A portion of this free amine (4.5 mg, 0.013 mmol) in DMF (0.2 mL) was added to a 4 mL vial containing [1-^{14}C]-*N*-BOC-Gly (1.5 mg, 0.0085 mmol), treated with *i*-Pr_2NEt (2 μL) and a solution of EDCI (5.0 mg, 0.026 mmol) in CH_2Cl_2 (0.1 mL), and stirred for 3 h at 25 °C. The reaction mixture was diluted with EtOAc (2.0 mL), washed with 10% aqueous HCl (3 × 1.0 mL), saturated aqueous Na_2CO_3 (1.0 mL), and saturated aqueous NaCl (1.0 mL), and evaporated. PTLC (SiO_2, EtOAc/$CHCl_3$ 1:1) provided 1.8 mg (41%) of **[^{14}C]-31** as a white film.

A 4 mL vial containing **[^{14}C]-31** (1.8 mg, 3.5 μmol) was treated with 4 N HCl−dioxane (0.25 mL) and the reaction stirred for 0.5 h at 25 °C. Solvent and excess acid were evaporated under a stream of N_2, and the resulting crude hydrochloride salt was treated with isophthaloyl dichloride (355 μg, 0.0018 mmol) in CH_2Cl_2 (0.1 mL) and *i*-Pr_2NEt (2.4 μL, 0.014 mmol) in CH_2Cl_2 (0.05 mL). After 3 h at 25 °C, the reaction mixture was directly purified by PTLC (SiO_2, MeOH/$CHCl_3$/EtOAc 1:9:9) to provide 1.2 mg (71%) of **[^{14}C]-33**.

A solution of **[^{14}C]-33** (1.2 mg, 1.2 μmol) in THF−MeOH (0.2 mL, 1:1) was treated with a solution of LiOH·H_2O (0.4 mg) in H_2O (0.05 mL) at 0 °C and stirred for 1 h. The reaction mixture was diluted with MeOH (1.0 mL), treated with Dowex 50WX-8 acidic cation-exchange resin (200 mg), and stirred for 1 min. The mixture was then filtered through cotton wool and the filtrate evaporated to provide 1.1 mg (94%) of **[^{14}C]-34**, relative activity approximately 110 mCi/mmol. This compound and all its synthetic intermediates were identical to the corresponding unlabeled material.

Solid Phase Integrin Binding Assays. Integrin binding assays were performed as described previously.[13] Briefly, purified integrins were adsorbed onto microtiter wells (1−5 μg/mL, 50 μL/well) overnight at 4 °C. Plates were washed to remove unbound integrin and blocked with 1% Caseinblocker (Pierce, Rockford, IL) for 1 h at 37 °C. Purified biotinylated MMP2 (bMMP2) in binding buffer (50 mM Tris pH 8, 150 mM NaCl, 1 mM $MgCl_2$, 1 mM $CaCl_2$, 0.5 mM $MnCl_2$) was added to the wells at a concentration of 3−5 nM in the presence or absence of compounds, or buffer vehicle alone. As a control, blocked wells without integrin were examined for binding as well. Biotinylated vitronectin (bVN; 1 μg/mL) was used as a reference for binding assays. After 90 min of binding at 37 °C, wells were washed extensively with binding buffer, and bound bMMP2 was detected with an HRP-labeled anti-biotin mAb. Antibody complexes were visualized with the single reagent peroxidase substrate TMB (BioRad, Hercules, CA), and the reaction was stopped with 0.18 M H_2SO_4. Binding was quantitated on a Kinetic Microplate Reader (Molecular Devices, Sunnyvale, CA).

For the assessment of direct integrin binding by **19**, purified integrin $\alpha_V\beta_3$ (10 μg/mL, 50 μL/well) was coated onto Immulon-4 microtiter wells (Dynatech Laboratories, Inc., Chantilly, VA), which were subsequently blocked as above and incubated with a titration of [^{14}C]-labled **19** prior to the addition of a 150 μL binding buffer containing 0.1% Tween-20 and aspiration of all liquid. Dried wells were separated and immersed in BetaMax liquid scintillation cocktail (ICN, Costa Mesa, CA) for quantitation. From this binding curve a subsaturating concentration (3 μM) of [^{14}C]-labeled **19** was chosen for inhibitor studies in the presence or absence of a 25-fold molar excess of unlabeled **19** or **9**, or 1 equiv of cyclic RGD peptide *c*(RGDfV).[21] Biotinylated vitronectin was used as a control and detected colorimetrically with HRP-conjugated anti-biotin mAb as described above.

Acknowledgment. This work was supported by the National Institutes of Health (D.L.B.; CA78045 and D.A.C.; CA45726 and CA50286) and the award of predoctoral (J.G.; NDSEG, 1995−1998) and postdoctoral (S.S.; NCI NRSA 1F32 CA72192-01; T.K.; Mildred-Scheel-Stipedium by Deutsche Krebshilfe) fellowships.

Supporting Information Available: Synthesis and characterization of compounds **35**−**41** and the structures of the complete set (77) of **1**, **A6B10C4** analogues containing modifications to R^2 (**1**, **A6B11C4-A6B87C4**). This material is available free of charge via the Internet at http://pubs.acs.org.

JA003579+